CHAPTER IV

RESULTS AND DISCUSSION

Ent–kaur-16-en-19-oic acid (Compound **1**) was used as a substrate for biotransformation process using *P. cubensis* as a biocatalyst. At the end of the biotransformation process, three products were obtained. The first product is *ent*-16β,17 dihydroxy-kauran-19-oic (Compound **2**), the second is *ent*-12α,16β,17-trihydroxy-kauran-19-oic acid (Compound **3**) and the third is *ent*-11α,16β,17-trihydroxy-kauran-19-oic acid (Compound **4**). For 2-days incubation, compound **2** was isolated and for a further 9-days incubation, compound **2**, **3** and **4** were isolated as the products. Compounds **3** and **4** were identified as novel compounds and the biological activity of all products were evaluated. Further more, due to the specificity of 16β,17 hydroxylation of *P. cubensis*, the enzyme involve in biotransformation was studied. The details of this research will be described as in the following sections.

4.1 The results of biotransformation of kaurenoic acid by *P. cubensis*

The substrate, *ent*-kaurenoic acid, was added into the late log period of cultures as describe in 3.5. The growth rate of the fungus is shown in Figure D1. The metabolites were monitored every two days by TLC using $CHCl_3$: CH_3OH (4:1) as solvent system and the chromatogram was compared with the control experiments. The chromatogram of TLC was showed in Figure 17. The chromatogram of the first two days incubation showed a compound with equal R*f* value as substrate (R*f* = 0.86) and one spot lower with a difference R*f* value of R*f* = 0.57, Compound **2**, when comparison with that of substrate and control experiments. It is indicated that a transformed product has been produced and its polarity was higher than that of *ent*-kaurenoic acid inferred by the higher R*f* value.

For the future cultivation period, two metabolites (Compound **3** and **4**) were detected. Compound **3** (R*f* = 0.41) and compound **4** (R*f* = 0.31) were detected on the third day of incubation and both spots appeared darkest on the ninth day of incubation while the spot of compound **2** still appeared but lighter than that which was found on the second day of incubation. At the end of incubation time, compound **1** has also

been found. From the results described above, it is investigated that *P. cubensis* is able to transformc **1** to form the three higher polar metabolites compound **2**, **3** and **4**. Compound **2** was reached the maximum quantity within two day after adding the substrate. Compound **3** and **4** were detected after 3 days of incubation and reached their the maximum quantity after cultivation for 9 days. Therefore, the production time of compound **2**, **3** and **4** is incubated for 2 and 9 days, respectively. Due to the remaining of compound **1** in the culture, it is suggested that the fungus can not transform all of the substrate added into the culture under these experimental condition. This might be the reason from the excess of substrate added.

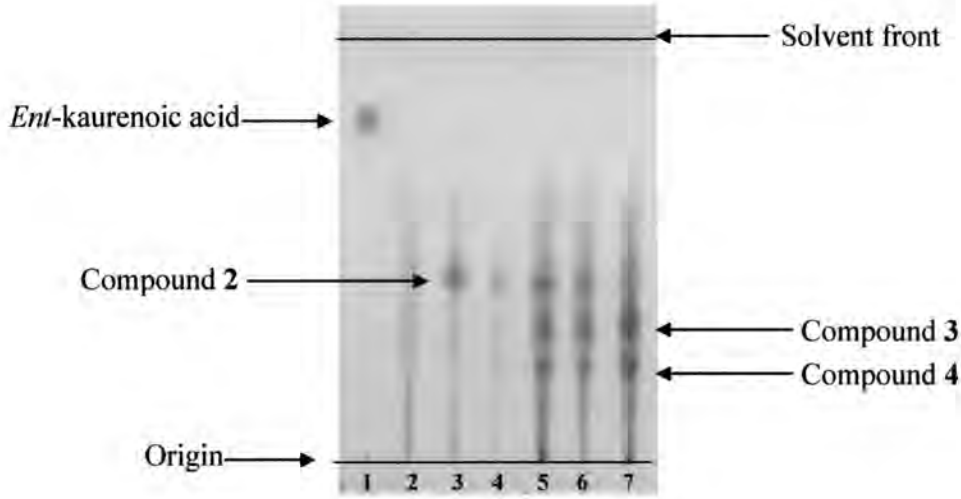

Figure 17. Chromatogram of product monitoring;

solvent system: $CHCl_3$: CH_3OH (4:1)

1 = *ent*-kaurenoic acid

2 = Crude EtOAC from *P. cubensis* culture without Compound **1**

3 = Crude EtOAC from 2 days incubation

4 = Crude EtOAC from 4 days incubation

5 = Crude EtOAC from 6 days incubation

6 = Crude EtOAC from 8 days incubation

7 = Crude EtOAC from 10 days incubation

4.2 The result of extraction process

4.2.1 Separation of 2-days incubation experiment

The viscous brown oil was obtained from ethyl acetate crude extract after evaporation. The crude extract was fractionated by silica gel column chromatography using silica gel 60 Art. 1.07734.10000 (230-400 mesh ATMS) as absorbent. The column was eluded with hexane-ethyl acetate and ethyl acetate-methanol gradient in a stepwise fashion to give compound **1** (20 %) and **2** (21.1 %) at 30% and 60% hexane in ethyl acetate, respectively. The structure of compound **2** was characterized by comparison of its NMR spectra with that of the authentic substrate.

4.2.2 Separation of 9-days incubation experiment

The viscous brown oil from 9-days incubation was extracted and purified by the same procedure as describe above. The column chromatography was eluded with hexane-ethyl acetate and ethyl acetate-methanol gradient in a stepwise fashion to give compound **1** (19.8 %) and compound **2** (11.5 %) at 30% and 60% hexane in ethyl acetate, respectively. In addition, compound **3** (8.3%) and compound **4** (2.8 %) were obtained when eluted with ethyl acetate and 5% methanol in ethyl acetate, respectively. The structures of all metabolites were characterized by spectroscopic methods and the spectral data were compared with the authentic substrate.

4.3 Structure elucidation of compound 2

Characterization of compound 2

Compound **2** was isolated as colorless powder. The IR spectrum of compound **2** (Figure C3) showed the broad absorption band between 3678 to 3068 cm^{-1} that correlated to the carboxylic and hydroxyl groups and the strong absorption band at 1696 cm^{-1} due to the carboxylic acid carbonyl stretching. The absorption bands of compound **2** are summarized in Table 4.

Table 4. The IR absorption bands assignment of Compound **2**

Wave number (cm^{-1})	Intensity	Vibration
3678-3068	broad	O-H stretching vibration of acid
2943	strong	C-H stretching vibration of $-CH_3$, CH_2
1696	strong	C=O stretching vibration of acid
868	medium	C-H out of plane bending vibration

The molecular structure of compound **2** indicated by comparison of its spectrometric data with those of the original substrate. The ^{1}H-NMR spectrum of compound **2** (Figure C5, Table 5) showed the two methyl group signals at 1.21 and 1.01 ppm indicated that the two methyl groups still existed. Moreover, it showed the absence of the unsaturated exocyclic methylene signal at 4.74 and 4.8 ppm, but presented the new signals of AB system at δ 3.74 and δ 3.63 (2H, *J*=11.2 and 11.6 Hz, respectively).

The ^{13}C-NMR (Figure C6, Table 5) showed 20 lines. From the ^{13}C-NMR and HSQC-NMR spectral data indicated the presence of two methyl carbons at 14.9 and 28.1 ppm, nine methylene carbons at 18.2, 18.9, 21.9, 25.9, 36.8, 37.8, 40.5, 41.9 and 52.3 ppm, three methine carbons at 44.8, 55.9 and 56.6 ppm and one methylene carbon of primary alcohol at δ 65.4 ppm. Three quaternary carbons appeared at δ 43.2, 44.4 and 39.4 ppm. and a quaternary carbon of tertiary alcohols appeared at δ 81.5 ppm. A signal at 180.2 ppm assigned for carbonyl group of carboxylic acid also appeared.

The mass spectrum showed the molecular weight as follows, m/z LC-MS (rel.int.) (Figure C4): 359 $(M+Na)^+$.

Assignment of the mass spectroscopic data of compound **2**, *m/z* = 336 and the respective sodium adduct at *m/z* = 359, was consistent with the molecular formula of $C_{20}H_{30}O_4$. This inferred that the two hydroxyl group were introduced into the original substrate (*m/z* = 302). Accordingly, the data suggested compound **2** as dihydroxylated kaurenoic acid.

The information from 2D-NMR techniques: HMBC correlation (Figure 18 and C9, Table 6), HSQC correlation (Figure C8, Table 5), COSY correlation (Figure 19 and C7, Table 6) and NOSY correlation (Figure C10) were used to characterize the structure of compound **2**.

The ^{13}C-NMR of Compound **2** comparison with that of compound **1** (Table 7), ^{1}H-NMR, its mass spectroscopic data and all information from 2D-NMR techniques confirmed compound **2** as 16,17-dihydroxylated.

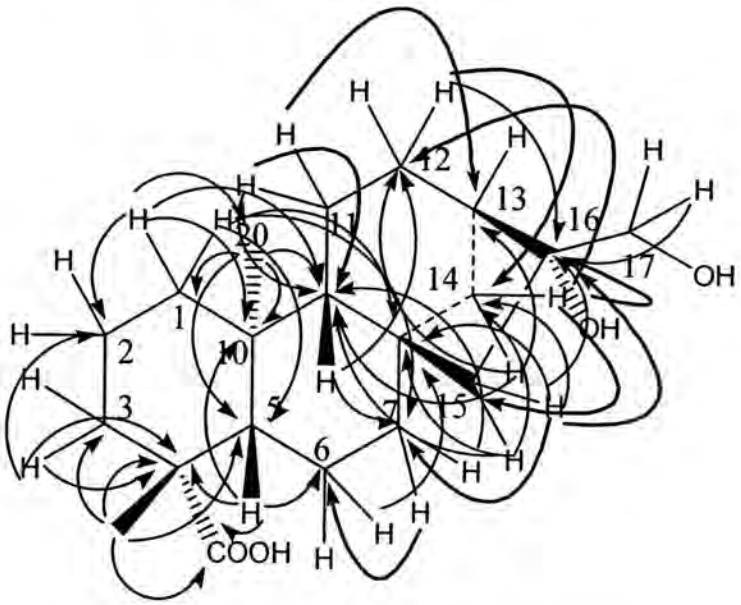

Figure 18. HMBC correlation of compound **2**

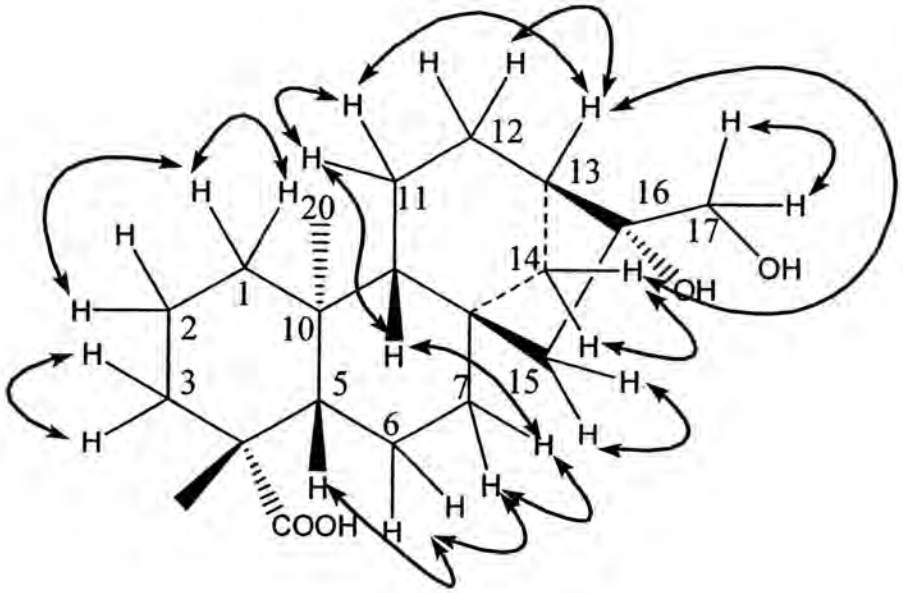

Figure 19. COSY correlation of compound **2**

Table 5. The HSQC spectral data of compound **2**

^{13}C-NMR (ppm)	^{1}H-NMR (ppm), coupling constant (Hz)
14.8	1.01s
18.2	1.54-1.67m
18.9	1.43br, 1.94br
21.9	1.81-1.90m
25.9	1.52m, 1.64m
28.1	1.21s
36.8	1.68m, 1.95d (*J*=12)
37.8	1.43m, 2.15brd (*J*=13.6)
39.4	-
40.5	0.86dt (*J*=3.6, 13.2), 1.89m
41.9	1.49m, 1.65m
43.2	-
44.4	-
44.8	2.05brs
52.3	1.42d (*J*=14.8), 1.56d (*J*=14)
55.9	1.04m
56.6	1.10dd (*J*=6,8.4)
65.4	3.63d (*J*=11.2), 3.74d (*J*=11.6)
81.5	-
180.2	-

Table 6. The HSQC, HMBC and COSY spectral data of compound **2**

Position	δ_C	δ_H	HMBC (H to C)	COSY
1	40.5	0.86dt	C-2, C-9, C-10, C-20	H1(1.88), H2(1.43)
		1.88m	C-5, C-7, C-8, C-10	H1(0.86)
2	18.9	1.43br		H1(0.86)
		1.94br		-
3	37.8	1.05m	C-2, C-4	H3(2.15)
		2.15br	-	H3(1.05)
4	43.2	-	-	-
5	56.6	1.10dd	C-4, C-6, C-10, C-18	H6(1.85-1.90)
6	21.9	1.81-1.90m	C-8	H5(1.10), H7(1.49)
7	41.9	1.49m	C-6	H7(1.65)
		1.65m	C-9	H7(1.49,1.65), H9(1.05)
8	44.4	-	-	-
9	55.9	1.04m	C-12	H11(1.61) (1.45-1.167)
10	39.4	-	-	-
11	18..2	1.54-1.67m	C-9, C-13	H11(1.67), H13(2.05), H14(1.95)
12	25.9	1.52m	C-8, C-14	-
		1.64m	-	H13(2.05)
13	44.8	2.05brs	-	H12(1.64), H14(1.68)
14	36.8	1.68m	C-9, C12, C-13	H13(2.05)
		1.95d	C-12, C-15, C-16	H14(1.68)
15	52.3	1.42d	C-8, C-9, C-14	H15(1.56)
		1.56d	C-7, C-8, C-9, C-14, C-16	H15(1.42)
16	81.5	-	-	-
17	65.4	3.63d	C-16	H17(3.63)
		3.74d	-	H17(3.64)
18	28.1	1.21s	C-3, C-4, C-5, C-19	-
19	180.2	-	-	-
20	14.9	1.01	C-1, C-5, C-9, C-10	H1(0.86)

Table 7. ^{13}C-NMR assignments for *ent*-kaur-16-en-19-oic acid (**1**) and compound **2** (400 MHz, CD_3OD, δ)

Position	δ_C (ppm)			
	Compound **1**	Compound **2**	Compound **2** (Silva et al., 1987)[a]	
			α16-	β16-
1	40.7	40.5	42.1	41.8
2	19.1	18.9	19.1	19.0
3	37.7	37.8	38.1	38.0
4	43.2	43.3	43.9	43.7
5	57.0	56.7	56.9	56.8
6	21.8	21.9	22.2	21.5
7	41.3	41.9	40.7	40.6
8	44.2	44.4	44.7	43.4
9	55.1	55.9	55.8	56.0
10	39.7	39.4	39.5	39.4
11	18.4	18.2	18.6	18.9
12	33.1	25.9	26.2	26.5
13	43.8	44.8	45.4	40.5
14	39.7	36.8	37.3	37.9
15	48.9	52.3	53.2	52.3
16	155.8	81.5	81.9	79.8
17	103.0	65.4	66.4	69.7
18	28.9	28.1	28.7	28.6
19	184.9	180.2	180.1	180.3
20	15.6	14.8	16.0	15.1

[a] 90.56 MHz, $CDCl_3$, δ in lit.

The stereochemistry at C-16 was deduced by comparison with the literature previously reported, the resonance of α and β-16,17-dihydroxy were presented at δ 81.6-81.8 and δ 79.8-79.8, respectively (Agrawal, Bishnoi and Singh, 1995). Thus, the chemical shift found for compound **2** at C-16 (δ 81.5) suggests the β-configuration for the 16 hydroxyl group (Table 7). Additionally, the comparison of melting point of compound **2** (261-263 °C) with the previously reported data which the temperature of 260-262 °C (Fraga et al., 1994). The result is in accordance with the assignment data of this report. In contradiction, the melting point of *ent*-16α,17 dihydroxy-kauran-19-oic acid was reported at 296-300 °C (Herz and Kulanthaival, 1984). Furthermore, the structure of compound **2** was investigated with regard to its optical rotation, $[\alpha]^{20}_{D}$ -65 ° (c 0.01, MeOH) in comparison with the former reports. The optical rotation of α and β-16,17-dihydroxy were reported previously at $[\alpha]^{24}_{D}$ -58 ° (*c* 0.05, CH_3OH) (Chang et al., 1998) and $[\alpha]^{24}_{D}$ -160 ° (*c* 0.02, CH_3OH) (Wu et al., 1996), respectively. The result indicated that the optical rotation of compound **2** correlated to α-16,17-dihydroxy. Therefore, over all data indicated that the hydroxyl was located at the α- position leading to the overall structure of e*nt*-16,17 dihydroxy-kauran-19-oic acid. Thus, it can be concluded that compound **2** is e*nt*-16β,17 dihydroxy-kauran-19-oic acid (Figure 20).

Compound **2**, e*nt*-16α,17 dihydroxy-kauran-19-oic acid, was found to be described in previous report as the compound which has been isolated from many plants; *Stevia paniculata* (Yamasaki et al., 1976), *Helianthus* sp. (Herz and Kulanthaival, 1984) *Annona recticulata* (Etse, Gray and Waterman et al., 1987), *Siegesbeckea pubescens* (Jiang, Yunbao and Yunlong, 1992), and *Cussonia bojeri* (Harinantenaian, Kasai and Yamaski, 2002). In the case of biotransformation, it was also found as the product from the biotransformation of *ent*-16α,17-epoxykauran-19-oic acid by *Gibberella fugikuroi* after incubation for 2 days (Fraga et al., 1994). Furthermore, in previous report on biotransformation of *ent*-kaurenoic acid, Silva and coworker have described compound **2** was isolated as the product from the biotransformation process by *R. stolonifer* after 15 days of incubation (Silva et al., 1999). In comparison with those biotransformation processes, the biotransformation of *ent*-kaurenoic acid by *P. cubensis* is better than those processes due to the fact that *ent*-kaurenoic acid is easier to obtain in large amount than 16β,17-epoxykauran-19-oic

acid and the incubation time is shorter than that of modification using *R. stolonifer*. Moreover, the previous literature reported that compound **2** can also be obtained from the chemical reaction (Etse et al., 1987). The reaction was started by treating kaurenoic acid in Et_2O and pyridine with OsO_4 at 0 °C for 24 h. The reaction mixture was diluted with Et_2O and treated with a solution of mannitol and KOH in H_2O. The mixture was refluxed for 2 h, and the organic layer was evaporated off to leave a residue which was washed with 5% HCl and H_2O. Column chromatography of the residue over Si gel 60 eluting with EtOAc to give *ent*-16β,17 dihydroxy-kauran-19-oic acid. By the comparison of chemical reaction and biotransformation, it is indicated that the one step biotransformation can shorten of this step in chemical reaction to produce the product, compound **2**, including with the chemical reagents have not been used. The last reason is leading to the environmental and energy saving.

The biological activity of compound **2** has been evaluated that its structure is related to the compound with the significant inhibition of HIV reverse transcriptase. *Ent*-16β,17dihydroxy-kauran-19-oic acid gave 46 % of inhibition against HIV reverse transcriptase at concentration 33 μg/ml (Chang et al., 1998).

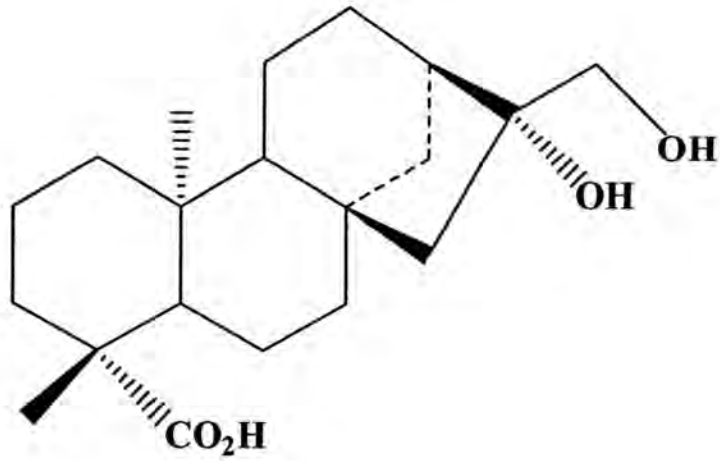

Figure 20. The structure of Compound **2**

4.4 Structure elucidation of compound 3

Characterization of compound 3

The IR spectrum of compound 3 (Figure C11) showed the broad absorption band between 3667 to 3052 cm^{-1} that correlated to the carboxylic and hydroxyl groups and the strong absorption band at 1679 cm^{-1} due to the carboxylic acid carbonyl stretching. The IR spectrum of compound **3** is summarized in Table 8.

Table 8. The IR absorption bands assignment of compound **3**

Wave number (cm^{-1})	Intensity	Vibration
3667-3052	broad	O-H stretching vibration of acid
2932	strong	C-H stretching vibration of $-CH_3$, CH_2
1679	strong	C=O stretching vibration of acid
862	medium	C-H out of plane bending vibration

The molecular structure of compound **3** indicated by comparison with the spectrometric data of the original substrate. The ^{1}H-NMR spectrum of compound **3** (Figure C14, Table 9) showed the signals at 1.21 and 1.01 ppm correlated to the two methyl groups. It also showed the absence of the olefinic proton signals as same as the spectrum of compound **2** and presented the new signals of AB system at δ 3.89 and δ 3.64 (2H, *J*=12.0 and 12.0 Hz, respectively).

The mass spectrum showed the molecular weight as follow, m/z LC-MS (rel.int.) (Figure C12): 374.9 $(M+Na)^+$ and HRESIMS m/z: 375.2149 (calcd for $C_{20}H_{32}O_5Na$, 375.2147) (Figure C13)

Assignment of the mass spectroscopic data of compound **3**, the respective sodium adduct at *m/z* = 375.2149 inferred the molecular weight of compound **3** is 352, consistent with the molecular formula of $C_{20}H_{32}O_5$. This inferred the three hydroxyl group were introduced into the original substrate (*m/z* = 302). Thus, the data suggests compound **3** to trihydroxylated kaurenoic acid.

The ^{13}C-NMR (Figure C15) showed 20 lines of carbon signals. From the ^{13}C-NMR and HSQC-NMR spectral data exhibit the presence of two methyl carbons at 15.0 and 28.1 ppm, eight methylene carbons at 18.9, 21.8, 27.9, 28.1, 36.1, 37.7, 40.5, 41.8 and 52.5 ppm, three methine carbons at 52.0, 56.4 and 56.5 ppm and one methylene carbon of primary alcohol at δ 67.1 ppm. Three quaternary carbons appeared at δ 38.9, 43.3 and 38.9 ppm. and two quaternary carbons of tertiary alcohols appeared at δ 70.1 and 81.4 ppm. A signal should be investigated for carbonyl group of carboxylic acid presented at 180.2 ppm.

The information from 2D-NMR techniques: HMBC correlation (Figure 21 and C18, Table 10), HSQC correlation (Figure C17, Table 9), COSY correlation (Figure 22 and C16, Table 10) and NOSY correlation (Figure 23 and C19) were used to characterize the structure of compound **3**.

Analysis of ^{13}C-NMR spectral data of compound **3**, compared to that of compound **1**, together with HMBC and HSQC correlation indicated the hydroxyl groups present at C-16 and C-17 (δ 81.4 and δ 67.1, respectively) as in compound **2**. Furthermore, the ^{13}C-NMR spectrum of compound **3** showed the new resonance of oxygenated carbon at δ 70.1 corresponding to C-12 this effected to downfield shift of the signals corresponding to C-11 (from δ18.4 to δ 27.9) and C-13 (from δ 43.8 to δ 52.0), as compared to that of compound **1**. These suggested that the hydroxyl groups were presented at C-12, C-16 and C-17.

The stereochemistry at C-12 was defined by the correlation from 2D-NOESY-NMR spectrum, the correlation was found between one proton of C-12 and the methyl proton at C-20. According to the overall data, compound **3** is suggested as *ent*-12α,16β,17-trihydroxykauran-19-oic acid.

Moreover, the structure and stereochemistry of compound **3** were confirmed by X-Ray crystallography. The ORTEP drawing of the molecule with relative configuration is given in Figure 25 and X-Ray diffraction data are presented in Tables D1, D2, D3 and D4, respectively.

The hydroxyl group at C-16 of compound **3** was identified as being located at the α-position. The related structural compound of **3** had been described in the literature (Gutierrez and Herz, 1990), on the occasion, the hydroxyl group at C-16 of this compound was suggested to be in the α-position, make this study is the first

report on *ent*-12α,16β,17-trihydroxy-kauran-19-oic acid. The chemical structure of compound **3** was shown in Figure 24.

Table 9. The HSQC spectral data of compound **3**

^{13}C-NMR (ppm)	^{1}H-NMR (ppm), coupling constant (Hz)
15.0	0.96s
18.9	1.46m, 1.93m
21.8	1.82m,1.85m
27.9	1.60m, 1.92m
28.1	1.22s
36.1	1.70m,1.88m
37.7	1.05dt (*J*=4.4,13.2), 2.16br
38.9	-
40.5	0.89m, 1.91m
40.8	1.52dd (*J*=4.0,12.8), 1.70m
43.3	-
44.1	-
52.0	2.21dd (*J*=4;12.8)
52.5	1.45d (*J*=14.4), 1.57d (*J*=14.4)
56.4	1.12 d (*J*=8.8)
56.5	1.18dd (*J*=2.4,11.6)
67.1	3.89d (*J*=12.0), 3.64d (*J*=12.0)
70.1	3.91br
81.4	-
180.2	-

Table 10. The HSQC, HMBC and COSY spectral data of compound **3**

Position	δ_C	δ_H	HMBC (H to C)	COSY
1	40.5	0.89m	C-2, C-20	H1(1.90)
		1.91m	C-9	H1(1.89)
2	18.9	1.46m	C-4	-
		1.93m	C-7	-
3	37.7	1.05dt	C-2, C-4, C-18	H3(2.16)
		2.16br	-	H3(1.05)
4	43.3	-	-	-
5	56.4	1.12 d	C-4, C-6, C-7, C-10, C-20	H6(1.82)
6	21.8	1.82m	-	-
		1.85m	-	H5(1.12)
7	40.8	1.52dd	C-14	-
		1.70m	-	H7(1.52), H15(1.45)
8	44.1	-	-	-
9	56.5	1.18dd	C-7, C-10, C-11, C12, C-14, C-15	H11(1.60)
10	38.9	-	-	-
11	27.9	1.60m	C-9, C-10	H9(1.18), H11(1.92), H12(3.91)
		1.92m	C-8, C9, C-12	H11(1.60), H12(3.91)
12	70.1	3.91br	C-16	H(1.60,1.92), H13(2.21)
13	52.0	2.21dd	C-8, C-11,C-12, C-15,C-16	H12(3.91), H14(1.72), H17(3.89)
14	36.1	1.70m	C-7, C-8, C-9, C-12, C-13	H13(2.21), H14(1.88)
		1.88m	C-16	H14(1.72)
15	52.5	1.45d	C-7, C-8, C-9, C-16	H15(1.57)
		1.57d	C-8, C-14, C-17	H14(1.72, 1.88), H15(1.45)
16	81.4	-	-	-
17	67.1	3.89d	C-15, C-16	H17(3.89)
		3.64d	C-15	H17(3.64)
18	28.1	1.22s	C-2, C-3, C-4,C-5, C-19	-
19	180.2	-	-	-
20	15.0	0.96s	C-1, C-9, C-10	-

Table 11. ^{13}C-NMR assignments for *ent*-kaur-16-en-19-oic acid (**1**), compound **2** and **3** (400 MHz, CD_3OD, δ)

Position	δ_C (ppm)		
	Compound **1**	Compound **2**	Compound **3**
1	40.7	40.5	40.5
2	19.1	18.9	18.9
3	37.7	37.8	37.7
4	43.2	43.3	43.3
5	57.0	56.7	56.4
6	21.8	21.9	21.8
7	41.3	41.9	40.8
8	44.2	44.4	44.1
9	55.1	55.9	56.5
10	39.7	39.4	38.9
11	18.4	18.2	27.9
12	33.1	25.9	70.1
13	43.8	44.8	52.0
14	39.7	36.8	36.1
15	48.9	52.3	52.5
16	155.8	81.5	81.4
17	103.0	65.4	67.1
18	28.9	28.1	28.1
19	184.9	180.2	180.2
20	15.6	14.8	15.0

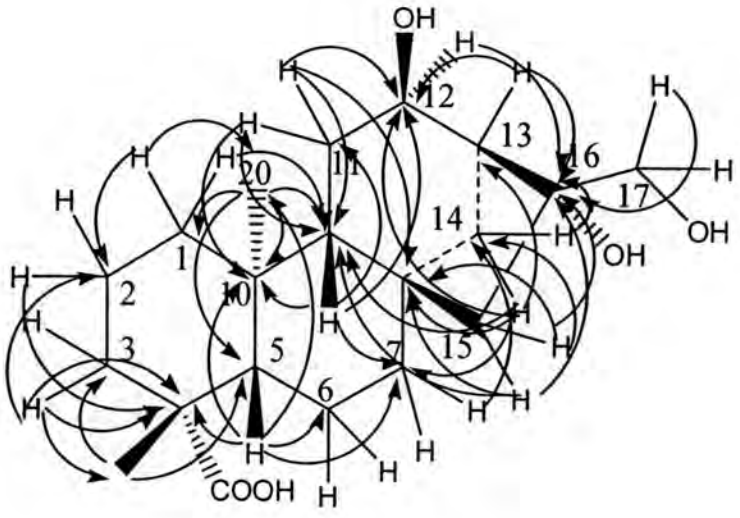

Figure 21. HMBC correlation of compound **3**

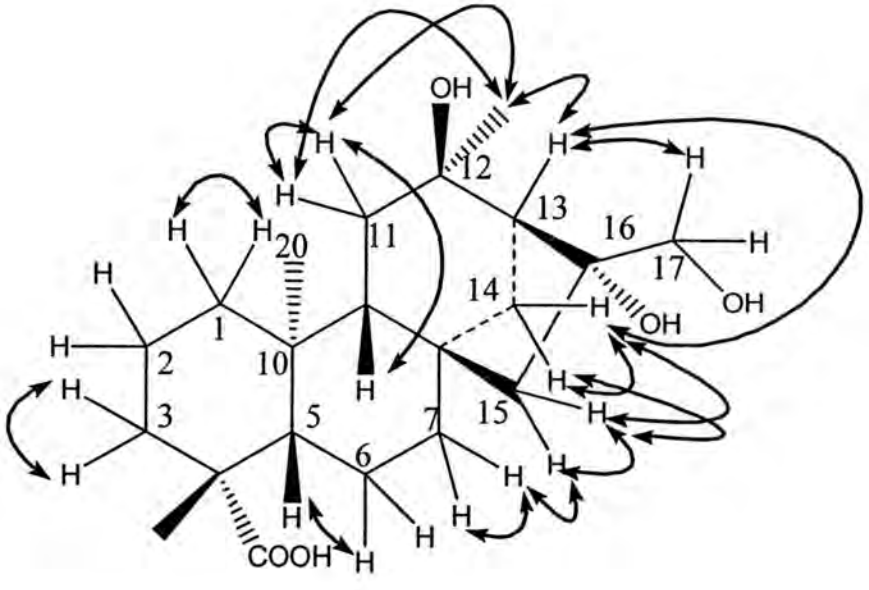

Figure 22. COSY correlation of compound **3**

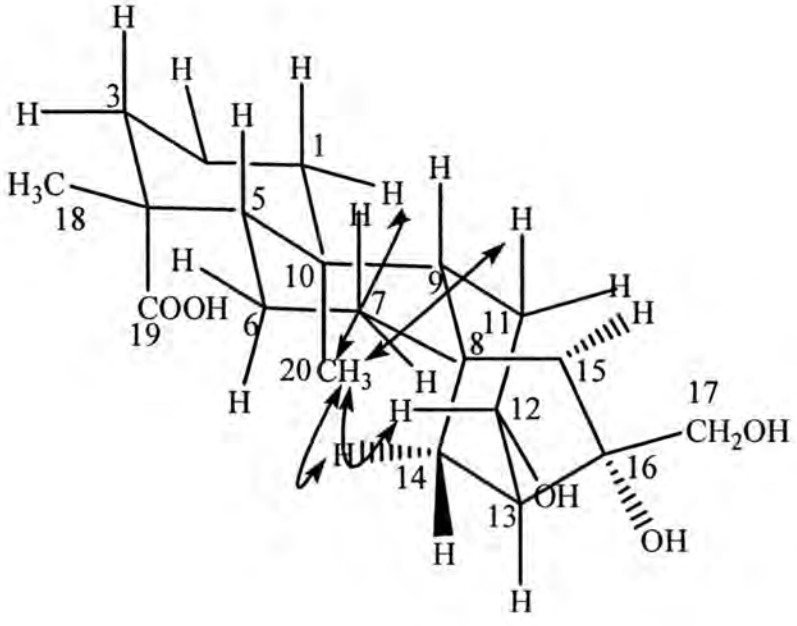

Figure 23. NOESY correlation of compound **3**

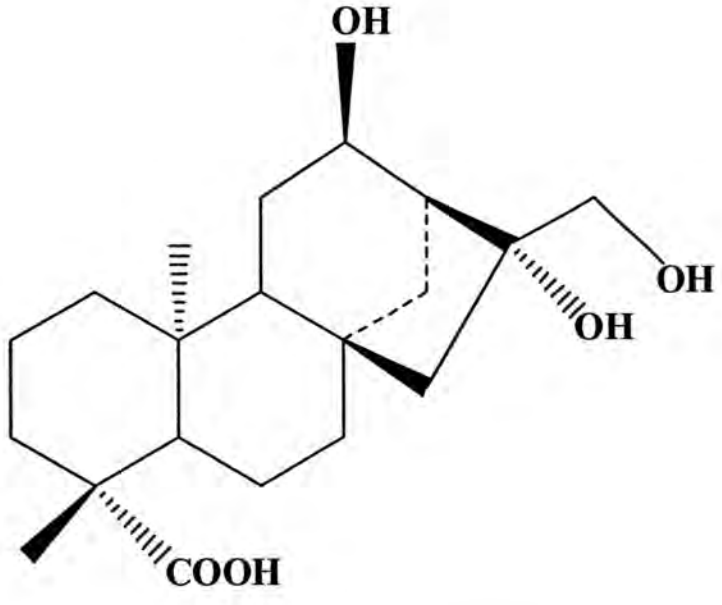

Figure 24. The structure of compound **3**

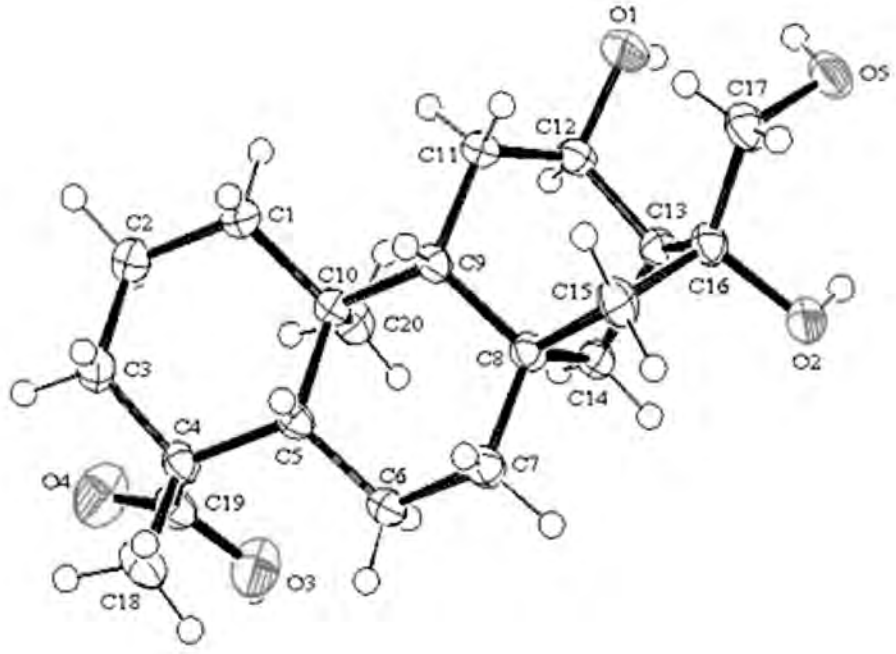

Figure 25. The computer generated ORTEP drawing of compound **3**

4.5 Structure elucidation of compound 4

Characterization of compound 4

The IR spectrum of compound **4** (Figure C20) showed the broad absorption band between 3657 to 3042 cm^{-1} that correlated to the carboxylic and hydroxyl groups and the strong absorption band at 1680 cm^{-1} due to the carboxylic acid carbonyl stretching. The IR spectrum of compound **3** is summarized in Table 12.

Table 12. The IR absorption bands assignment of compound **4**

Wave number (cm^{-1})	Intensity	Vibration
3657-3042	broad	O-H stretching vibration of acid
2941	strong	C-H stretching vibration of $-CH_3$, CH_2
1680	strong	C=O stretching vibration of acid
865	medium	C-H out of plane bending vibration

The molecular structure of compound **4** indicated by comparison with the spectrometric data of the original substrate. The ^{1}H-NMR spectrum (Figure C23, Table 13) of compound **4** showed the absence of the unsaturated exocyclic methylene signal as same as the spectrum of compound **2** and compound **3** and presented the new signals of AB system at δ 3.70 and δ 4.12 (2H, *J*=11.2 and 11.2 Hz, respectively).

The mass spectrum showed the molecular weight as follow, m/z LC-MS (rel.int.) (Figure C21 and C22): 375.1 $(M+Na)^+$ and HRESIMS m/z: 375.2154 (calcd for $C_{20}H_{32}O_5Na$, 375.2147).

Assignment of the mass spectroscopic data of compound **4**, the respective sodium adduct at *m/z* = 375.2154 inferred the molecular weight of compound is 352, consistent with the molecular formula of $C_{20}H_{32}O_5$. This inferred the three hydroxyl groups were introduced into the original substrate (*m/z* = 302). Thus, the data suggests compound **4** to be a trihydroxylated kaurenoic acid.

The ^{13}C-NMR (Figure C24, Table 13) showed 20 lines and presented the resonance of three oxygenated carbon atoms at δ 81.8, δ 65.9 and δ 64.8.

The ^{13}C-NMR showed 20 lines of carbon signals. From the ^{13}C-NMR and HSQC-NMR spectral data exhibit the presence of two methyl carbons at 14.1 and 28.1 ppm, eight methylene carbons at 18.8, 35.6, 35.9, 37.7, 39.6, 41.9, 50.3, and 69.9 ppm, three methine carbons at 35.9, 42.8 and 43.3 ppm and one methylene carbon of primary alcohol at δ 81.8 ppm. Three quaternary carbons appeared at δ 44.5, 56.5 and 64.9 ppm. and two quaternary carbons of tertiary alcohols appeared at δ 64.8 and 81.8 ppm. The signal presented at 180.2 ppm. should be assigned for carbonyl group of carboxylic acid.

The information from 2D-NMR techniques: HMBC correlation (Figure 26 and C27, Table 14), HSQC correlation (Figure C26, Table 13), COSY correlation (Figure 27 and C25, Table 14) and NOESY correlation (Figure 28 and C28) were used for characterize the structure of compound **4**.

The spectroscopic data of compound **4** suggested di-hydroxylation has occurred at the original 16-17 double bond and the C-16 configuration was observed as 16α-hydroxylation as compound **2** and **3**. The ^{1}H-NMR spectrum of compound **4** showed a new one proton signal centered at δ 3.85 (d, J = 6.8) corresponding to the resonance of C-11 at δ 64.8, from ^{13}C-NMR spectrum (Table 18), this indicates the occurrence of hydroxylation at C-11. The presence of the hydroxyl group at C-11 is reflected in a downfield displacement of the C-9 and C-12 signal at δ 64.9 and δ 35.6, respectively. The stereochemistry at C-11 was determined from the signal multiplicity of the corresponding proton and from the related structure compound previously described (Hanson, 1995). The NOESY experiment defined the β-configuration of the hydroxyl group at C-11 as a correlation was found between H-11 and one of the hydrogen at C-1 and between H-11 and the methyl proton at C-20. The results suggested the overall structure of compound **4** as *ent*-11α,16β,17-trihydroxykauran-19-oic acid (Figure 29). As the structure of this compound, the C-11 hydroxylation is of special interest; the hydroxylation at C-11 is required for the function at C-11 position of some steroidal hormone derivative (Vieira et al., 2002). Furthermore, compound **4** was identified as a new compound.

Table 13. The HSQC spectral data of compound **4**

^{13}C-NMR (ppm)	^{1}H-NMR (ppm), coupling constant (Hz)
14.4	0.87s
18.8	1.90m, 1.42br
21.7	1.80m
28.1	1.18s
35.6	1.73m, 1.98m
35.9	1.76m, 1.68m
37.7	2.11br, 1.04dt (*J*=4, 13.6)
38.3	-
39.6	1.93m, 1.09m
41.9	1.64m, 1.47m
42.8	-
43.3	-
44.5	2.03br
50.3	2.09d (*J*=14.4), 1.20d (*J*=14.4)
56.5	1.10m
64.8	3.85d (*J*=6.8)
64.9	1.18m
65.9	3.70d (*J*=11.2), 4.12d (*J*=11.2)
81.8	-
180.2	-

Table 14. The HSQC, HMBC and COSY spectral data of compound **4**

Position	δ_C	δ_H	HMBC (H to C)	COSY
1	39.6	1.09m	C-6, C-10	H1(1.92), H2(1.42), H20(0.87)
				H1(1.08), H2(1.42), H3(2.11)
		1.93m	-	
2	18.8	1.42br	C-4	H1(1.92), H3 (2.11)
		1.90m	-	H1(1.08), H2(1.42), H3 (2.11)
3	37.7	1.04dt	C-2	H3 (2.11)
		2.11br	-	H2(1.42, 1.90), H3(1.036)
4	43.3	-	-	-
5	56.5	1.10m	C-6, C-7, C-10, C-18, C-20	H6(1.81, 1.96)
6	21.7	1.80m	C-8, C-10	H5(1.10), H7(1.47)
7	41.9	1.47m	C-14	H6(1.81), H7(1.66)
		1.64m	C-14	H6(1.81), H7(1.47)
8	42.8	-	-	-
9	64.9	1.18m	C-1, C-8, C-11, C-20	H12(1.73), H20(0.87)
10	35.9	-	-	-
11	64.8	3.85d	C-8, C-9, C-10, C-12, C-13	H12(1.73)
12	35.6	1.73m	C-11, C-13, C-14	H11(3.86), H12(1.97), 13(2.03)
		1.98m	C-13	H12(1.73)
13	44.5	2.03br	-	H12(1.73)
14	35.9	1.68m	C12, C-13	H14(1.78), H13(2.03)
		1.78m	C-8, C-9,C-12, C-13, C-15	H14(1.68)
15	50.3	1.20d	C-3, C-7, C-9, C-16	H15(2.09)
		2.09d	C-8, C-9, C-14	H15(1.27)
16	81.8	-	-	-
17	65.9	3.70d	C-13, C-15, C-16	H17(4.13)
		4.12d	C-13, C-15, C-16	H17(3.72)
18	28.1	1.18s	C-3, C-4, C-5, C-19	-
19	180.2	-	-	-
20	14.4	0.87s	C-1, C-5, C-9, C-10	H1(1.081), H9(1.19)

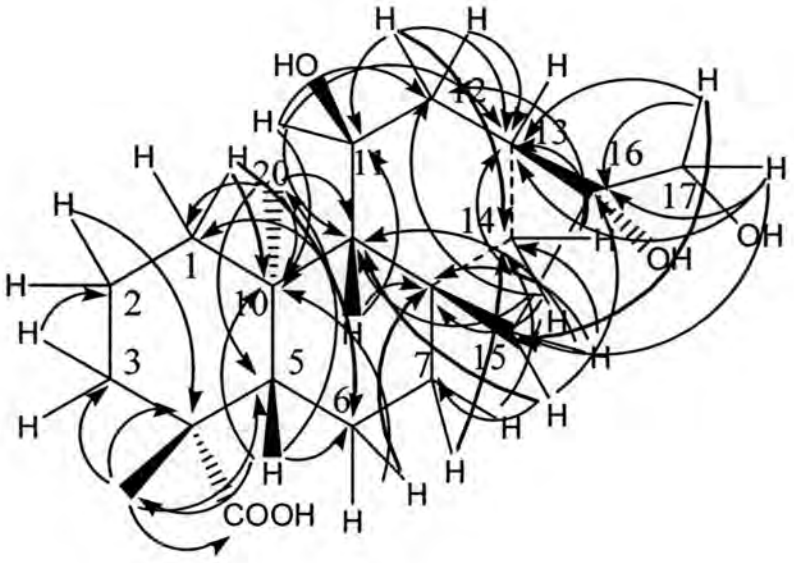

Figure 26. HMBC correlation of compound **4**

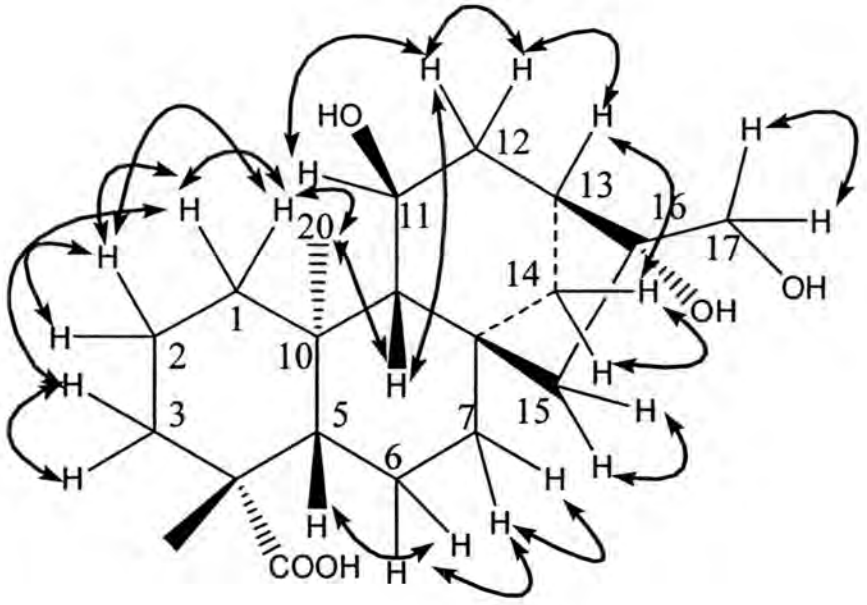

Figure 27. COSY correlation of compound **4**

Table 15. ^{13}C-NMR assignments for *ent*-kaur-16-en-19-oic acid (**1**) and compound **2** and **4** (400 MHz, CD_3OD, δ)

Position	δ_C (ppm)		
	Compound **1**	Compound **2**	Compound **4**
1	40.7	40.5	39.6
2	19.1	18.9	18.8
3	37.7	37.8	37.7
4	43.2	43.3	43.3
5	57.0	56.7	56.5
6	21.8	21.9	21.7
7	41.3	41.9	41.9
8	44.2	44.4	42.8
9	55.1	55.9	64.9
10	39.7	39.4	38.3
11	18.4	18.2	64.8
12	33.1	25.9	35.6
13	43.8	44.8	44.5
14	39.7	36.8	35.9
15	48.9	52.3	50.3
16	155.8	81.5	81.8
17	103.0	65.4	65.9
18	28.9	28.1	28.1
19	184.9	180.2	180.2
20	15.6	14.8	14.4

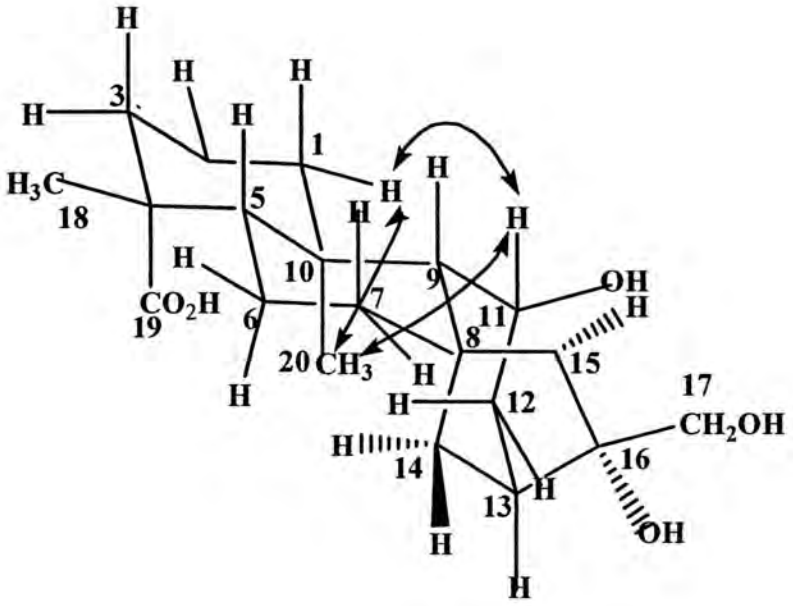

Figure 28. NOESY correlation of compound **4**

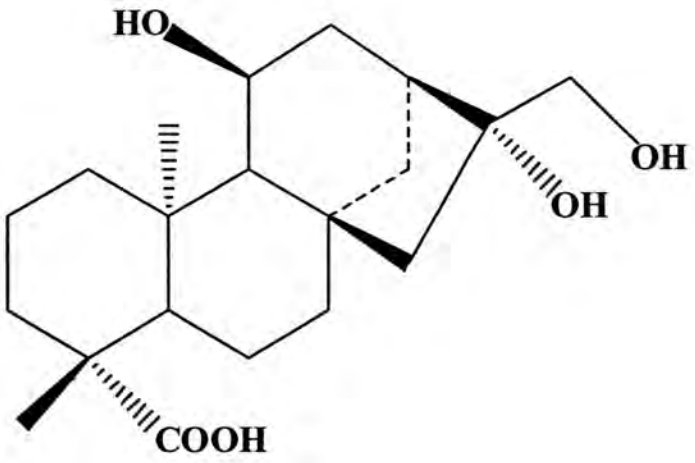

Figure 29. The structure of compound **4**

4.6 Epoxidation of compound 1

Compound **1** (200 mg, 0.66 mmol) was epoxidise with m-CPBA ($C_7H_5ClO_3$, 120 mg, 0.69 mmol, 1:1 eq) in dichloromethane for 5 hours to give compound **1a** (40 mg, mmol, %). The path way for epoxidation of compound **1** is shown in Scheme 5. By comparison of the NMR spectra with the former report, the result indicated compound **1a** as 16,17-epoxy-kauran-19-oic acid.

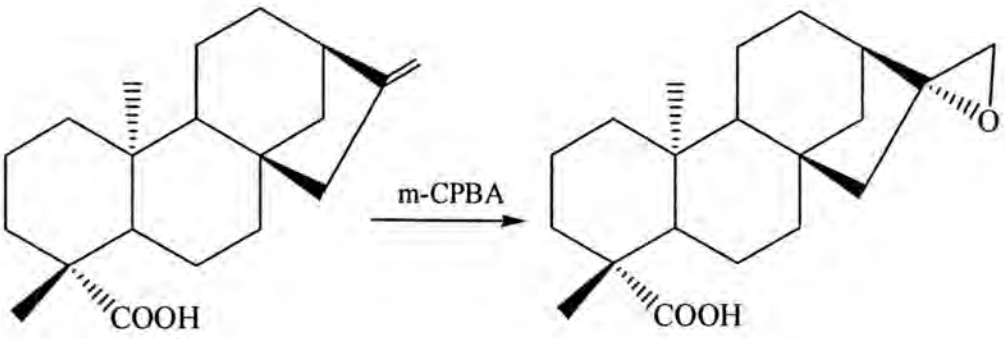

Compound **1** Compound **1a**

Scheme 5. The epoxidation of compound **1**

The structure elucidation of compound **1a** was performed by comparison of the NMR spectra with the literature previously described (Sirimongkhon, 2000). The ^{1}H-NMR spectra of compound **1a** is shown in Figure C28.

4.7 Biotransformation of Compound 1a

Compound **1a** was added into the 5 days old culture of *P. cubensis*. After 2 days of incubation, the culture was extracted with EtOAc and removed the solvent by the rotary evaporator under reduce pressure. The crude extract was examined by TLC using $CHCl_3$: MeOH (4:1) as solvent system. The chromatogram has also been compared with the product of *ent*-kaurenoic biotransformation, compound **2**, **3**, and **4** (Figure 30.). The result reveal that compound **1a** has been transform to be compound **2** by *P. cubensis* after incubated for 2 days. The control experiment without microorganism showed the result that compound **1a** was not changed without the

microorganism. These results suggested that compound **1a** was transformed to be the compound **2** by the enzyme system in *P. cubensis*.

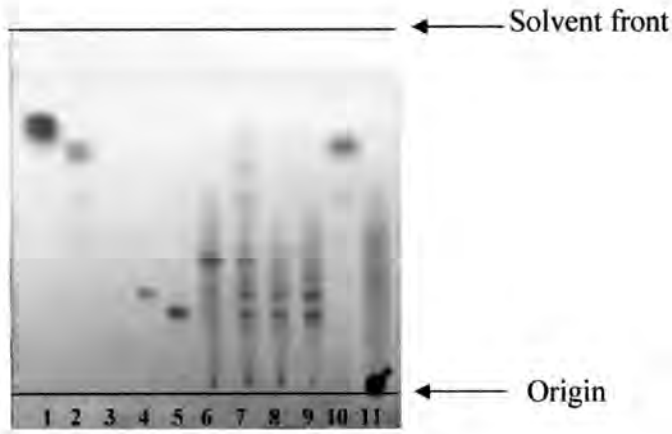

Figure 30. The chromatogram of biotransformation of compound **1a** by *P. cubensis*; solvent system: $CHCl_3$: CH_3OH (4:1)

1 = *ent*-kaurenoic acid
2 = Compound **1a**
3 = Compound **2**
4 = Compound **3**
5 = Compound **4**
6 = Crude EtOAC from 2 days incubation
7 = Crude EtOAC from 4 days incubation
8 = Crude EtOAC from 6 days incubation
9 = Crude EtOAC from 9 days incubation
10 = Crude EtOAC from compound **1a** in media without *P. cubensis*
11 = Crude EtOAC from *P. cubensis* culture without compound **1a**

4.8 Biotransformation of compound 2

After incubation of compound **2** with *P. cubensis* for 9 days, the cultures were extracted with EtOAc and the solvent was removed. The crude extract was applied on TLC for comparison with compound **2**, **3**, and **4**. The chromatogram is shown in Figure 31. The chromatogram revealed that incubation of compound **2** with *P. cubensis* resulted in compound **3** and **4**. For the control experiment without the fungus, compound **2** was found in the medium without any other metabolites. It is clear that compound **3** and **4** were produced by the enzyme system in *P. cubensis*.

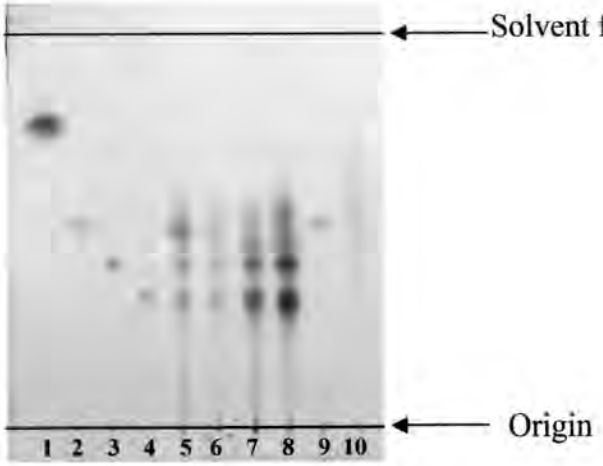

Figure 31. The Chromatogram of biotransformation of compound **2** by *P. cubensis*; solvent system: $CHCl_3$: CH_3OH (4:1)

1 = *ent*-kaurenoic acid
2 = Compound **2**
3 = Compound **3**
4 = Compound **4**
5 = Crude EtOAC from 2 days incubation
6 = Crude EtOAC from 4 days incubation
7 = Crude EtOAC from 6 days incubation
8 = Crude EtOAC from 9 days incubation
9 = Crude EtOAC from compound **2** in media without *P. cubensis*
10 = Crude EtOAC from *P. cubensis* culture without compound **2**

4.9 The possible pathway of product formation

The production of compound **2** was studied by incubation of compound **1a** with *P. cubensis*. The experiment was set by the suspicious that the dihydroxy groups of compound **2** might be transformed and pass through the epoxide formation of *ent*-kaurenoic acid. In this study, compound **2** was isolated from the culture as the first product after 2 days incubation. The epoxide has not been detected in the culture but, normally, the possible metabolic pathway to form compound **2** has been proposed that pass through the epoxide formation. Previous literature reported that the epoxide is not stable in culture (Faber et al., 2001). It was transformed further to be the diol metabolite, this means the epoxide could not be found in the culture. It is possible that the transformation of compound **1** to compound **2** by *P. cubensis* pass through the formation of *ent*-16β,17-epoxy-kauran-19-oic acid and then transform to be compound **2**. To prove this, the 16,17-epoxykaurenoic acid (Compound **1a**) was synthesized and seeded into the culture of *P. cubensis*. The results showed compound **1a** has been transform to be compound **2** by *P. cubensis* whereas the control experiment revealed the structure of compound **1a** has not been changed without the fungus. For the further incubation for 9 days, the chromatogram on TLC showed the same pattern as the biotransformation which using *ent*-kaurenoic acid as the substrate.

In according with the previous literature, the incorporation of *ent*-kaurenoic acid into the derived hydroxyl acid and dihydroxy acid has been studied in the plant *Beyeria calycina* (Croft, Ghisalberti and Jefferies, 1978). In this report, the 16,17 diol kaurenoic acid was performed and the possibilities of the mechanism were summarized in Scheme 6. By this scheme, it was shown that the epoxide was required for the formation of the dihydroxy acid before it is transformed to the other metabolites.

Furthermore in 1994, the microbiological transformation of two *ent*-16β,17-epoxy-kauran-19-oic acid was performed by the fungus *G. fujikuroi* affording two metabolites, *ent*-16β,17-dihydroxykaurenoic acid and 16α,17-dihydroxygibberellin A_{12} (Figure 32) (Fraga et al., 1994). This study showed the 16β,17-dihydroxy-kaurenoic acid afforded from the starting material,16β,17-epoxy-kauran-19-oic acid, by the biotransformation using *G. fujikuroi*. Consideration from both studies suggests the production of 16,17-dihydroxykaurenoic acid is possible via the transformation of the epoxide. According to the literatures described above, they indicated that normally

the formation of *ent*-16β,17-dihydroxykaurenoic acid required the epoxide formation at C-16 and C-17 of *ent*-kaurenoic acid. This inferred that in this study the transformation of compound **1a** to compound **2** occurred via the enzyme system of *P. cubensis* and the possibility of the formation of compound **2** may required the epoxide formation to form 16β,17-epoxy-kauran-19-oic acid.

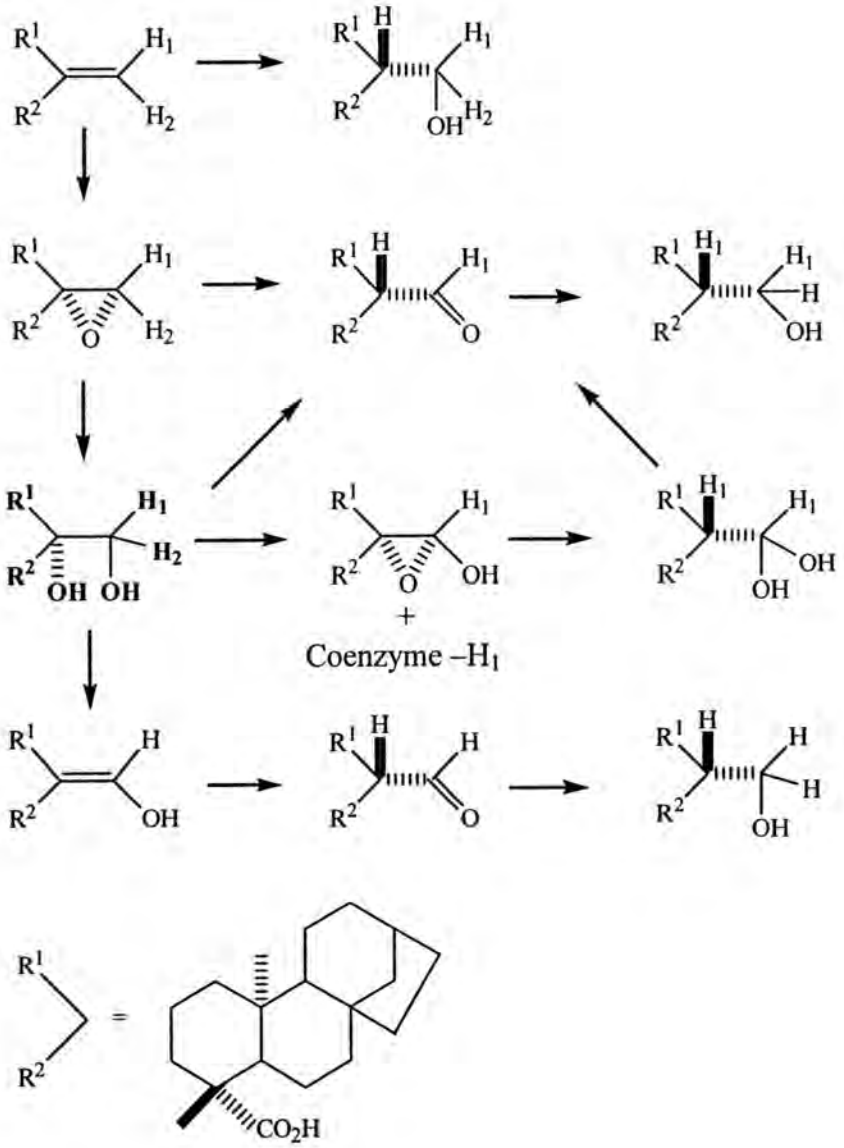

Scheme 6. The formation of hydroxyl acid and dihydroxy acid of *ent*-kaurenoic acid in *Beyeria calycina* (Croft et al., 1978)

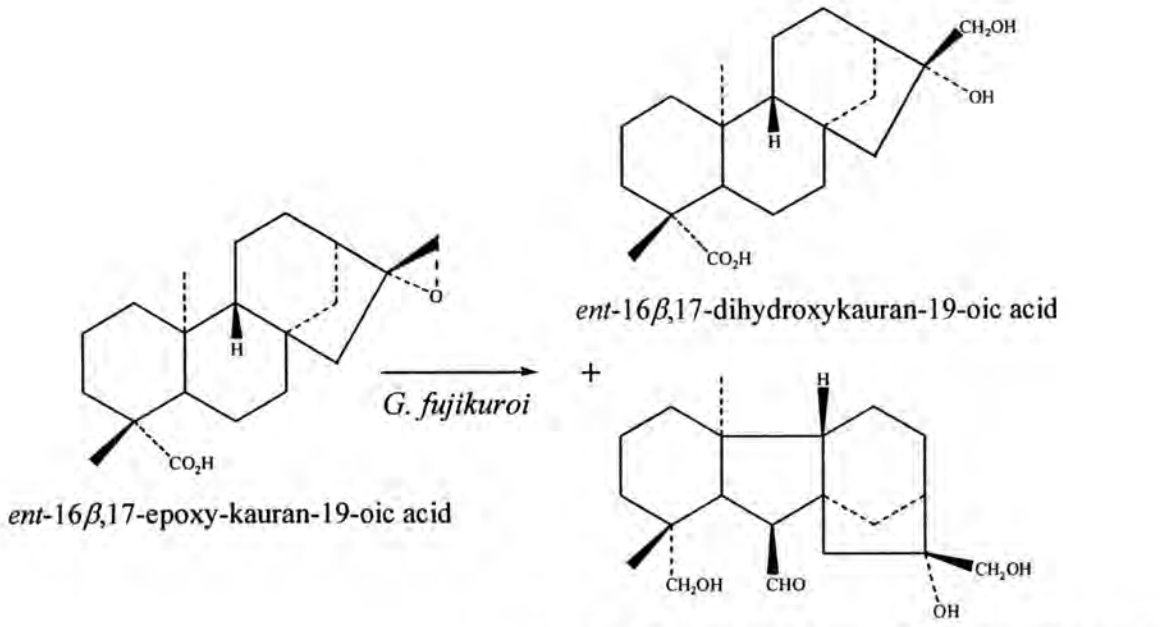

Figure 32. Biotransformation of *ent*-16β,17-epoxy-kauran-19-oic acid by the fungus *G. fujikuroi* (Fraga et al., 1994)

For the production of compound **3** and **4**, from the TLC products monitoring, the reduction of compound **2** whereas compound **3** and **4** was increasing after 2 days of incubation might indicate that the transformation of compound **2** to be compound **3** and **4**. In the experiment which used compound **2** as a substrate, in the same conditions, the control experiment showed the metabolite has not been changed without microorganism but when incubated with the fungus, compound **3** and **4** were detected. For the longer period of incubation, the chromatogram on the TLC showed the same pattern as the biotransformation which using *ent*-kaurenoic acid as the substrate.

The result suggested that compound **2** has been transformed to compound **3** and **4** by the enzyme system in *P. cubensis*.

From all over results, the metabolic pathway of biotransformation of *ent*-kauranoic acid by *P. cubensis* can be proposed as in Scheme 7.

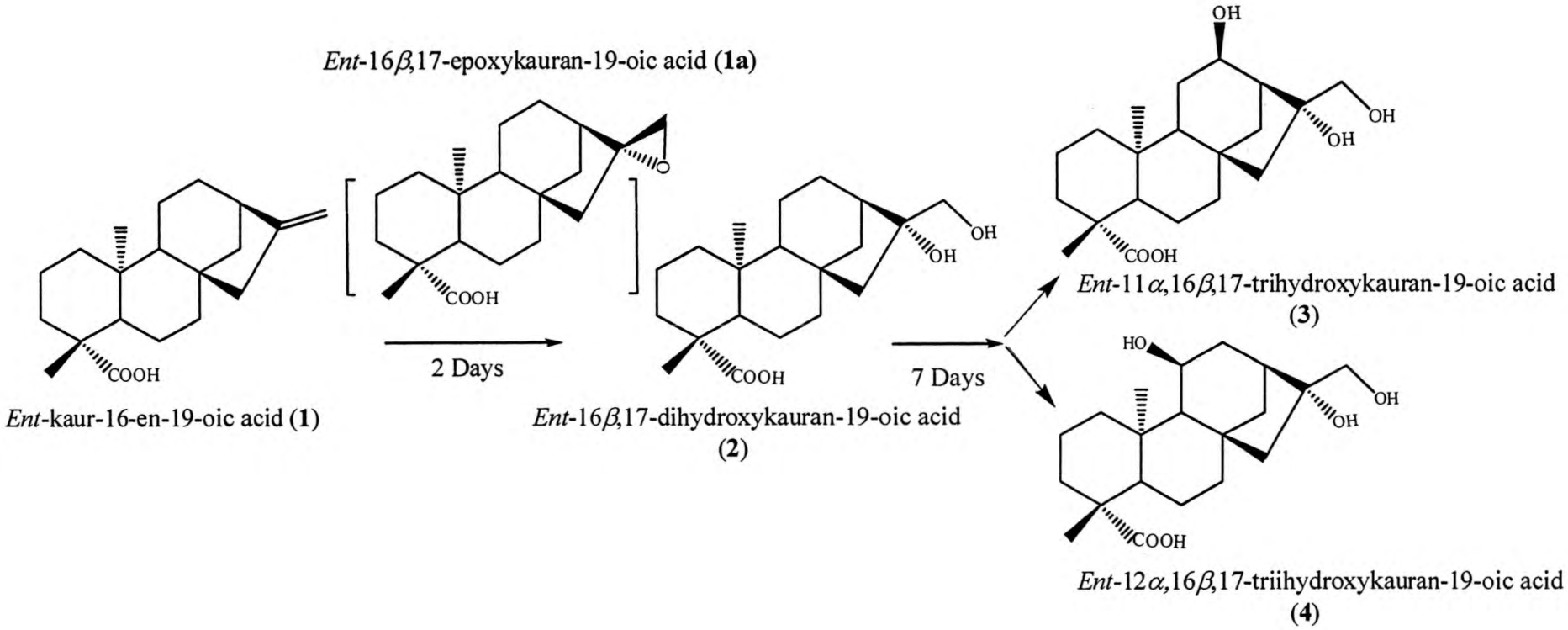

Scheme 7. The proposed pathway of biotransformation of *ent*-kaurenoic acid by *P. cubensis* ; the structure in brackets, 16β,17-epoxy-kauran-19-oic acid, cannot be detected.

4.10 Biological evaluation

4.10.1 Anti-microbial activity

The anti-bacterial activities were evaluated on four bacteria, *Bacillus cereus*, *Staphylococcus aureus* ATTC 25923, *Escherichia coli* ATTC 25922 and *Pseudomonas aeruginosa* ATTC 27853. The disc diffusion method were used for these evaluation, each disc contained 250 μg of metabolite. The results indicated that compound **2**, **3**, and **4** were inactive against all microorganisms accept compound **1** showed some activity against *Bacillus cereous* with the clear zone of 1.1 cm. Under the same conditions, Streptomycin and Chloramphenical showed the inhibition against all four organisms. This infers that the modification of C-16 and 17 of *ent*-kaurenoic acid cannot improve the anti- bacterial activity against the tested bacteria.

4.10.2 Cytotoxicity test

4.10.2.1 Cytotoxicity test on human tumor cell lines.

All metabolites were tested for cytotoxic activity towards 5 human tumor cell lines which contain HEP-G2 (hepatoma), SW620 (colon), Chago (lung), KATO-3 (gastric) and BT474 (breast) *in vitro*. The assay was performed by the MTT [3-(4,5-dimethylthiazol-2-yl)-2,5-diphenyltetrazolium bromide] colorimetric method. The results indicated that the metabolites except compound **1** were inactive against those five cell lines.

4.10.2.2 Antiproliferation on human erythromyeloblastoid leukemia cell line (K-562)

The result of antiproliferation assay toward K-562 cell line of compound **1**, **2**, **3**, and **4** are showed in Table 16.

Table 16. The antiproliferation assay on K-562 cell line of compound **1**, **2**, **3**, and **4**

Compounds	%*
Compound **1**	1.15 ± 1.35
Compound **2**	68.70 ± 3.81
Compound **3**	68.69 ± 2.40
Compound **4**	74.96 ± 2.72
Camthothecin	11.31 ± 6.23

* % = Cell viability (% of control)

The results indicated that compound **1** showed significant activity on antiproliferation of K-562 cell line at 1.15 % cell viability. Compound **2**, **3**, and **4** even at a high concentration (100 μg/mL) slightly inhibited K562 proliferation where cell viability remained at 68.70 ± 3.81%, 69.69 ± 2.40% and 74.96 ± 2.72 %, respectively ($p < 0.05$).

The results of biological activity evaluation of compound **2**, **3**, and **4**, consistently showed a much lower sensitivity of the cytotoxic test for all human tumor and human erythromyeloblastoid leukemia cell line than substrate, compound **1**. The reduction in activities of all products was considered by comparison of the chemical structure of compound **2**, **3**, and **4** with that of compound **1**. All products showed the different structure from compound **1** which presents the exocyclic double bond between C-16 and C-17. Compound **2**, **3**, and **4** are structurally similar except for the additional hydroxyl group at C-12 and C-11 of compound **3** and **4**, respectively. These results suggested that the structural modification at C-16 and C-17 to be 16α,17-dihydroxilated products lead to decrease in activity against all cell lines test. These results are in accordance with the report that suggested the presence of an exo-methylene group is important for the kaurane diterpenes for cytotoxic activity (Gui et al., 2004; Henry et al., 2006).

Although the biological activities which have been tested on compound **2**, **3** and **4** in this study were not active but the other interesting biological activity is anti-HIV activity. The anti-HIV activity of compound **2** was evaluated, it showed the

significant inhibition of HIV-reverse transcriptase (Chang et al., 1998). It is interesting to evaluated compound **3** and **4** on this activity.

4.11 Enzyme study

4.11.1 Constitutive and *ent*-kaurenoic acid-inducible oxygenase activities in mycelium

The enzyme activity of kaurenoic acid oxygenase was assayed in a noninduced (S_{10N}) and an induced (S_{10I}) fractions. The reduction of NADPH at 340 nm of each fraction was recorded (Figure 33) and the specific activities of each fraction are shown in Table 17. The enzyme activity of *ent*-kaurenoic acid oxygenase in the noninduced preparation was lower than that of the induced fraction. A comparison of the kaurene oxidase activities in crude (S_{10}) extracts showed that the extract of the induced fraction (S_{10I}) exhibited a 6.18-fold higher specific activity than that of the noninduced fraction (S_{10N}). The results indicated that the enzyme responsible for NADPH reduction in the presence of *ent*-kaurenoic acid is an inducible enzyme. Although, partial activity was also found in a control without substrate (the specific activity of 1.61 U/μg protein), this might be exerted by the substrate remaining in the fraction.

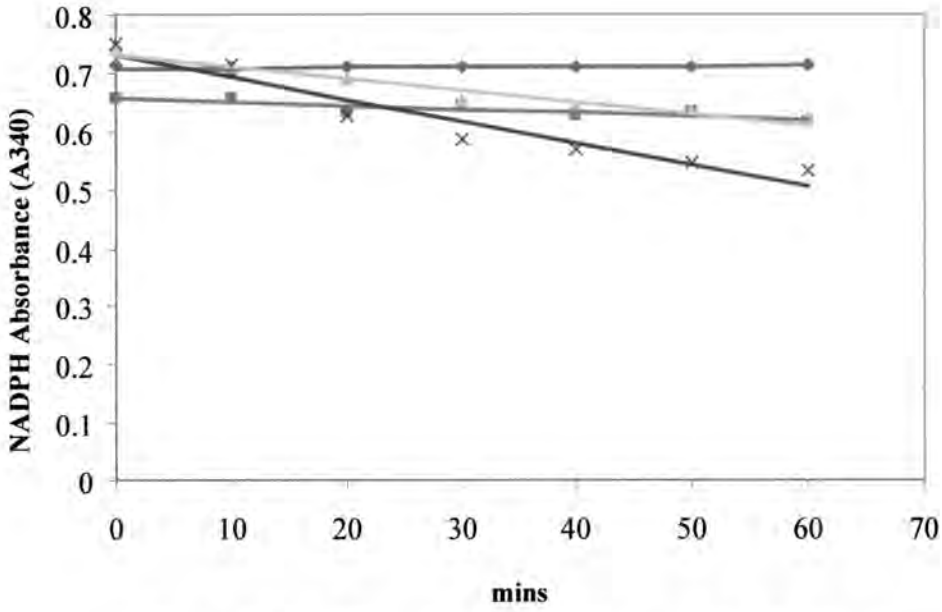

Figure 33. NADPH reduction rate of S_{10N} and S_{10I} fractions

- Non-induced fraction (S_{10N}) in the presence of 0.15 mM NADPH and 4 μM FAD, without *ent*-kaurenoic acid
- Non-induced fraction (S_{10N}) in the presence of 0.15 mM NADPH and 4 μM FAD, with 0.15 mM *ent*-kaurenoic acid
- Induced fraction (S_{10I}) in the presence of 0.15 mM NADPH and 4 μM FAD, without *ent*-kaurenoic acid
- Induced fraction (S_{10I}) in the presence of 0.15 mM NADPH and 4 μM FAD, with 0.15 mM *ent*-kaurenoic acid

Table 17. The activities of S_{10N} and S_{10I} fraction on *ent*-kaurenoic acid

Fractions*	U (μmol/min)	Specific activities (U/μg protein)
S_{10N}+NADPH+FAD+ *ent*-kaurenoic acid	96.5	0.48
S_{10N}+NADPH+FAD- *ent*-kaurenoic acid	ND	ND
S_{10I}+NADPH+FAD+ *ent*-kaurenoic acid	594.8	2.97
S_{10I}+NADPH+FAD- *ent*-kaurenoic acid	321.5	1.61

ND = Non Detected

* The reaction preparation is described in 3.9.2.1.

4.11.2 Localization of the enzyme

Cell extracts were sub-fractionated by centrifugation to yield crude (S_{10}), microsomal (P_{100}) and cytosolic (S_{100}) frations. The enzyme activities were investigated on the fractions, P_{100I}, and S_{100I}. The results are shown in Figure 35 and 36. From the enzyme activity assay, the specific activities are showed in Table 18.

After the disruption of the kaurenoic acid-induced mycelium, the suspension was separated by centrifugation at 10,000 x *g* and 100,000 x *g*, respectively. At 10,000 x *g*, the cell debris was discarded to obtain S_{10I} fraction which contain the intracellular fraction. Then, S_{10} was further separated at 100,000 x *g* to obtain the microsomal (P_{100I}) and cytosolic (S_{100I}) fractions. The P_{100I} and S_{100I} fractions were assayed for enzyme activity. The results showed the highest activity in the microsomal fraction. This indicated that the enzyme responsible for NADPH reduction associated with kaurenoic acid oxygenation was located in P_{100I} fraction. This inferred that the enzyme is localized at the intracellular site and the activity presented in the postmitocondrial supernatant is associated with the microsomal in the cell.

In S_{100I} fraction, the enzymes detected in the reaction with and without substrate were not significantly different, the results were shown in Table 18. This

result indicated that the enzyme in S_{100N} which found to reduce NADPH in the reaction mixture was not associated with *ent*-kaurenoic acid oxygenation.

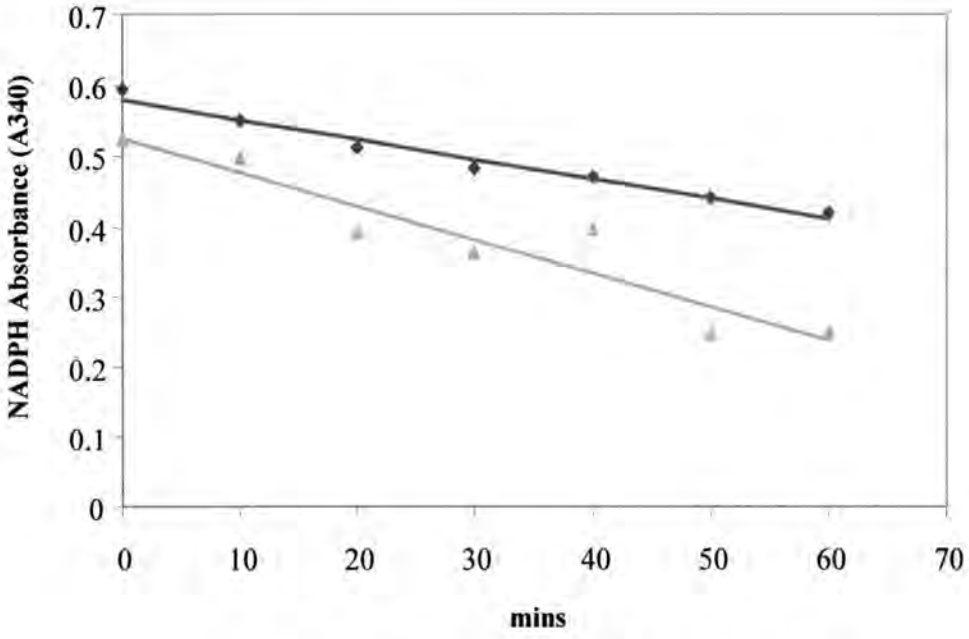

Figure 34. NADPH reduction rate of P_{100I} fraction

- Induced fraction (P_{100I}) in the presence of 0.15 mM NADPH and 4 μM FAD, without *ent*-kaurenoic acid
- Induced fraction (P_{100I}) in the presence of 0.15 mM NADPH and 4 μM FAD, with 0.15 mM *ent*-kaurenoic acid

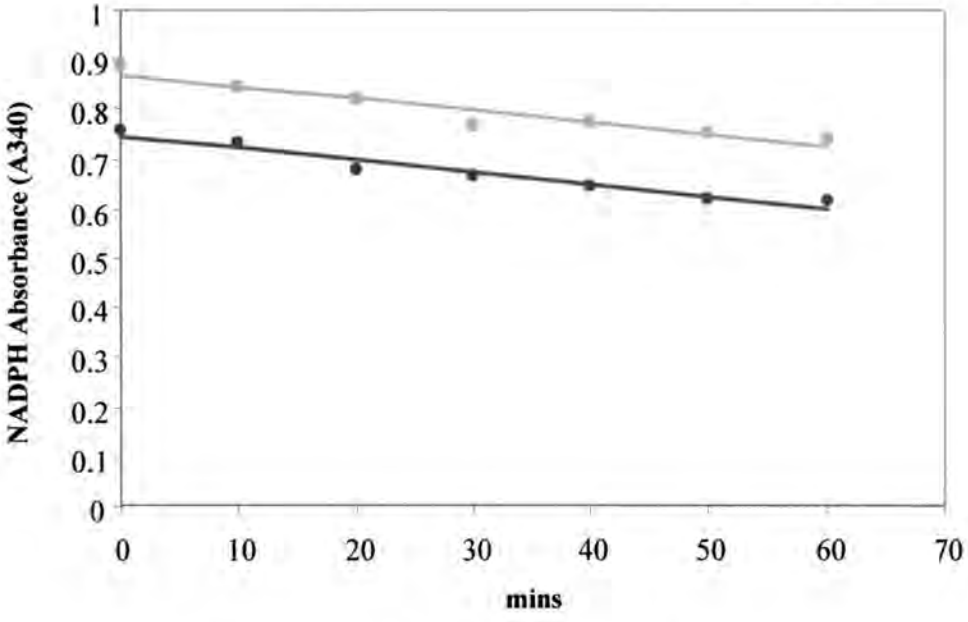

Figure 35. NADPH reduction rate of S_{100I} fraction

Induced fraction (S_{100I}) in the presence of 0.15 mM NADPH and 4 μM FAD, without *ent*-kaurenoic acid

Induced fraction (S_{100I}) in the presence of 0.15 mM NADPH and 4 μM FAD, with 0.15 mM *ent*-kaurenoic acid

Table 18. The activities of P_{100I} and S_{100I} fraction on *ent*-kaurenoic acid

Fractions*	U (μmol/min)	Specific activities (U/μg protein)
P_{100I}+NADPH+FAD+*ent*-kaurenoic acid	755.6	3.78
P_{100I}+NADPH+FAD- *ent*-kaurenoic acid	450.2	2.25
S_{100I}+NADPH+FAD+ *ent*-kaurenoic acid	385.8	1.92
S_{100I}+NADPH+FAD- *ent*-kaurenoic acid	385.8	1.92

* The reaction preparation is described in 3.9.2.1.

4.11.3 Assay of *ent*-kaurenoic acid activity in subcellular fraction

The assay was performed on subcellular fractions (P_{100I} and P_{100N}) incubated with *ent*-kaurenoic acid and enzyme cofactor, NADPH and FAD, for 60 min at 30 °C. Two control experiments were also performed. First, the sample was heated in boiling water for 10 min and, second, the reaction was carried out without add substrate. After the reaction was stop, each mixture was extracted with chloroform and applied on to the TLC. The chromatogram is shown in Figure 36.

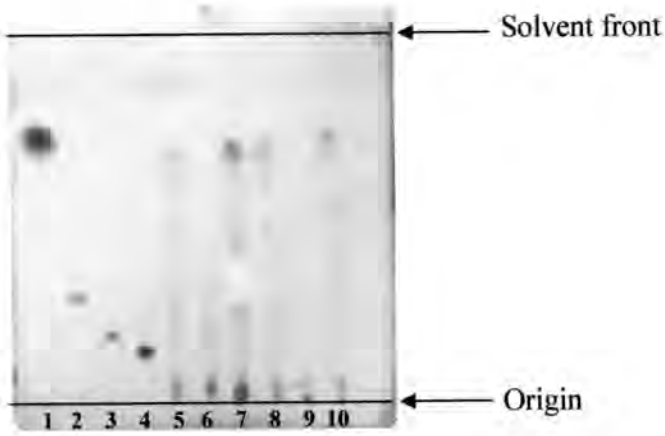

Figure 36. The chromatogram of *ent*-kaurenoic acid activity in subcellular fraction solvent system: $CHCl_3$: CH_3OH (4:1)

1 = *ent*-kaurenoic acid
2 = Compound **2**
3 = Compound **3**
4 = Compound **4**
5 = P_{100I} + Substrate
6 = P_{100I} - Substrate
7 = P_{100I} (heat) + Substrate
8 = P_{100N} + Substrate
9 = P_{100N} - Substrate
10 = P_{100N} (heat) + Substrate

The chromatogram showed that substrate and compound **2** was detected in every induced subcellular fraction including the control group.Thus this experiment cannot be used to assay the activity of *ent*-kaurenoic acid oxygenase. From the previous reports, the experiments were successful for assays the kaurenoic acid hydroxylase by using radioactive labeled substrate such as *ent*-[^3H]-kaurene

(Ashman, Mackenzie and Bramley, 1990) or [^{14}C]-kaurenoic acid (Jenning et al., 1993). These methods makes the allow of the biotransformation process to be detected and evaluated for their quantity.

4.11.4 The influence of cofactor on enzyme activity

The experiments were performed on P_{100I} fraction. The results are showed in Table 19.

Table 19. Effect of cofactor on enzyme activity

Cofactor	Specific activity (U/μg protein)
Non	ND
NADPH	1.29
NADPH+FAD	3.74

ND = Non Detected

The enzyme activities were observed on P_{100N} fraction. The activity of the enzyme was increased by 2.90 fold when NADPH (0.15 mM) was provided. None the less, the activity was increased more if the combination of NADPH and FAD were added into the reaction. The combination of NADPH and FAD in the reaction was stimulatory, as shown by the activities of P_{100I} in Table 19. The results suggested that using FAD as the cofactor together with NADPH can improve the activity of this enzyme up to 2.9-fold. Both cofactors are typically required for oxygenase enzyme, and have been reported to be essential for kaurene oxidase activity in plant and microorganism cell extract (Ashman et al., 1990).

The results of the enzyme study concluded that this enzyme is inducible, NADPH dependent and located in the microsome. Although, the results cannot indicate that the direct responsibility of the enzyme toward compound **2** production, the inducibility of the enzyme is correlated with the *ent*-kaurenoic acid oxidation.

4.12 MALDI-MS and Protein Identification

The cell fractions from induced (S_{10I}) and non-induced (S_{10N}) mycelium from 10,000 g centrifugation were separated in 12.5% SDS polyacrylamide gel electrophoresis as described in section 3.9.6. Standard protein was run in parallel and after electrophoresis, proteins were stained with Coomassie brilliant blue. The SDS-PAGE is showed in Figure 37.

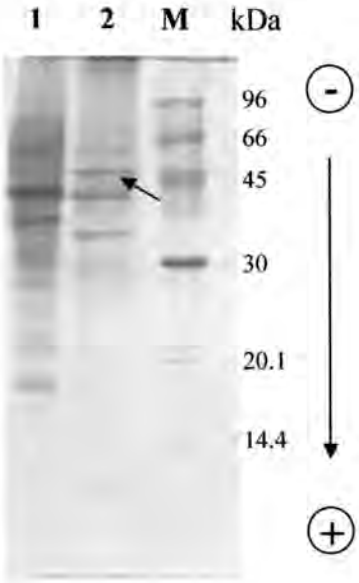

Figure 37. SDS-PAGE analysis of S_{10N} and S_{10I} on a 12.5% acrylamide gel

Lane **M** = Standard molecular weight protein

Lane **1** = S_{10N} (noninduce preparation)

Lane **2** = S_{10I} (induced preparation)

From SDS-PAGE, 5 bands of protein in the molecular weight range of 30-96 kDa were selected for digestion with trypsin and identified by MALDI/Tof MS and peptide mass fingerprinting database searching. Among them, the band which is indicated with an arrow (Figure 37) was analyzed by peptide mass fingerprinting. The results showed that the peptide matched to the Cyt P450 monooxygenase of the fungus *Aspergillus fumigatus* Af293 at the sequence coverage at 12 %. The matched peptide fragments were shown as follow;

Matched peptides shown in **bold texts**

1 MDFLQRILGI LSSEDVAPAL FASSISVLFL ILSYQVLYPP SKYSAFPTIN
51 GTRWLALSNR RILAEFVTDA QGLMRNGLEK YDIFRIISSI PMTILHPKY
101 TDEIHNDRQL NFMAVLAKEM FPNYPGFDLF REGTDGSTVL DAVK**FGSSR**
151 **CLGK**STQLLS DETSTLLQKL WGDEPEWHEV TAKSSVHDII HLSALLFYG
201 PELCSHKEWL EVTDEYASVG FLAARQLRLW PPILRPIAQW LPACRRLRY
251 LASRTRGLIE PVIAARQK**EK AICYSHGR**QP PVYDDAIEWT RAAKGRPYD
301 AAMSPLLFSI NALHTTTDLL TQVILDLSTQ PDLIVALRQE LSVKPQQNG
351 WKNASLNQLL LMDSAIKESQ R**LKPTESILM RRYAMDDLTL DGNKIPK**GT
401 VLGIPIFGMR **DPKIYVDPDM YDGYRFQK**MR DKPGFENKCQ VSTSPWHLG
451 FGHGIHACPG RFLAAVQVKI ILCYIVAKYD FKLAGGAPPK QSVGIELIS
501 DTEARLAVRR RQEMVIGLE

The result showed that the peptide fragment was matched to Cyt P450 monooxygenase of the fungus *Aspergillus fumigatus* Af293 but at a low percentage of sequence coverage. This might be because the number of peptide fragments is not enough for analysis. Moreover, it is possible that protein data from *P. cubensis* is not sufficient in the database. This result suggested that the enzyme intentatively Cyt P450 monooxygenase. To improve the experiment and to confirm the finding, more concentrations and peptide fragments would be provided for further analysis. Moreover, the other methods should be performed to identify the Cyt P450 such as the enzyme inhibitor assay and the spectral characteristic of Cyt P450 (Ashman et al., 1990; Jenning et al., 1993).

According to the results from biotransformation process, the proposed pathway of this biotransformation and the enzyme studies suggested that the enzyme which is responsible in the biotransformation of *ent*-kaurenoic acid to form compound **2** is probably the Cyt P450 monoxygenase which catalyzes the epoxide formation between the unsaturated C-atom, C-16 and C-17, of kaurenoic acid. The Cyt P450 monooxygenase has previously been reported as the enzyme system which catalyze the epoxidation of the unsaturated carbon group of the substrate (Holland, 1992). The production of epoxidase by biotransformation of unsaturated substrates are beneficial on providing a method for stereospecific preparation of the functional group that are superior in term of the relative and absolute stereochemistry to any known chemical

procedure as shown in this experiment. Additionally, the previous literature reported that the cytochrome P450 of eukaryotic organisms are all bound to the membranes of endoplasmic reticulum or mitochondria and required NADPH and/or FAD/FMN as cofactors (Omura, 1999; Urlacher, Lutz-Wahl and Schmid, 2004; Warrilow et al., 2002). In our experiments, the results indicated that the enzyme is located in the microsomal fraction suggesting the membrane protein and NADPH and FAD were both required for activity. These results support theoretically that the enzyme is Cyt P450.